International Journal of Mechanical, Industrial and Aerospace Sciences
ISSN: 2517-9950
Vol:12, No:9, 2018

Pilot Induced Oscillations Adaptive Suppression in Fly-By-Wire Systems

Herlandson C. Moura, Jorge H. Bidinotto, Eduardo M. Belo

***Abstract*—**The present work proposes the development of an adaptive control system which enables the suppression of Pilot Induced Oscillations (PIO) in Digital Fly-By-Wire (DFBW) aircrafts. The proposed system consists of a Modified Model Reference Adaptive Control (M-MRAC) integrated with the Gain Scheduling technique. The PIO oscillations are detected using a Real Time Oscillation Verifier (ROVER) algorithm, which then enables the system to switch between two reference models; one in PIO condition, with low proneness to the phenomenon and another one in normal condition, with high (or medium) proneness. The reference models are defined in a closed loop condition using the Linear Quadratic Regulator (LQR) control methodology for Multiple-Input-Multiple-Output (MIMO) systems. The implemented algorithms are simulated in software implementations with state space models and commercial flight simulators as the controlled elements and with pilot dynamics models. A sequence of pitch angles is considered as the reference signal, named as Synthetic Task (Syntask), which must be tracked by the pilot models. The initial outcomes show that the proposed system can detect and suppress (or mitigate) the PIO oscillations in real time before it reaches high amplitudes.

***Keywords*—**Adaptive control, digital fly-by-wire, oscillations suppression, PIO.

I. Introduction

THE advent of Fly-By-Wire (FBW) systems allowed a wide range of aircraft flight control system architectures. The integration of a digital computer to those systems in a configuration named DFBW enabled also the implementation of different flight dynamics to be followed by the aircrafts. These dynamics can be represented through different methodologies such as the stability and control derivatives. Nevertheless, those systems inherited some undesired aircraft responses from the manual flight control systems such as the called PIO. This phenomenon is commonly defined as inadvertent oscillations initiated and sustained by the pilot resulting in a pilot-aircraft coupling [1]. The big challenge of this undesired event resides in the fact that it cannot be always avoided, and it can be detected only when the oscillations start. Despite the great number of works performed since the 1960s, as [2]-[4], this phenomenon still occurs, threatening the flight of commercial and military aircraft since its occurrence can lead to severe aircraft accidents. The issue of finding an adequate algorithm can perform a real time detection of the phenomenon, and especially its suppression (or mitigation) remains open. Furthermore, few researches were conducted using the adaptive control theory to suppress the phenomenon in the DFBW systems. Considering this scenario, the present work proposes the development and implementation of an adaptive control system which performs the suppression of the PIO oscillations. The unsteady motion of interest is the longitudinal dynamics, so the PIO oscillations occur in the pitch motion. The PIO cause factors are considered to be: the rate and position actuators limiting, the high pilot gain and the time delays of the system. A secondary objective of the present work is finding a set of models, based on the stability and control derivatives methodology, with low and high proneness for the PIO phenomenon to be applied in the development of the algorithm.

The paper is organized as follows: Aircrafts Dynamics Models are presented in Section II, followed by the description of the control system developed in Section III, including the ROVER algorithm and the pilot models considered. Next, the methodology applied in the simulations is described in Section IV. The results and a discussion about them are presented in Sections V and VI, respectively. Lastly, the last section presents some concluding remarks with possible future works.

II. Aircraft Dynamics Models

An aircraft can be modelled as a rigid body with six degrees of freedom, three for translation (along the *x, y* and *z* axes) and three for rotational motion (*roll (ϕ), pitch (θ)* and *yaw (ψ)*). In the flight dynamics formulation, it is usual to define an airframe stability axes O_B located at the aircraft's center of gravity (CG), which follows its movement as presented in Fig. 1. This frame is referenced to another reference frame O_E. Once these airframes axes are defined, the resultant aerodynamic forces can be divided in three components [*X,Y,Z*], each one acting along the corresponded axis. The resultant moment vector, correspondingly, has three components [*L,M,N*] representing the rolling, pitching and yawing moments, respectively. The velocity of the aircraft's CG can also be split in its components [*u,v,w*], which occurs similarly with the angular velocity with its components [*p,q,r*], which represents the rate of roll, pitch and yaw correspondingly. The linearized equations of aircrafts motion in the longitudinal plane can so be derived, taking into account some simplifying assumptions. Considering these

H. C. Moura is with the University of São Paulo, Engineering School of São Carlos, Brazil. Av. João Dagnone, 1100. 13563-120 (phone +55 16 3373-8350, e-mail: herlandsonc@usp.br) and supported by National Council for Scientific and Technological Development (CNPq).

J. H. Bidinotto is with the University of São Paulo, Engineering School of São Carlos, Brazil. Av. João Dagnone, 1100. 13563-120 (phone +55 16 3373-8350, e-mail: jhbidi@sc.usp.br) and supported by São Paulo Research Foundation (FAPESP), Grant 2016/16808-5.

E. M. Belo is with the University of São Paulo, Engineering School of São Carlos, Brazil. Av. João Dagnone, 1100. 13563-120. (phone +55 16 3373-8350, e-mail: belo@sc.usp.br).

simplifications and the Etkin [5] formulation, which applies the small-disturbance theory, the linear equations of longitudinal aircrafts motion can be defined as a state space model. In the present work, the variables reference values are represented by a zero subscript, whereas the small perturbations from the reference condition are denoted by the Δ prefix. In this formulation, the longitudinal aircraft dynamics can be then represented by the equations:

$$\dot{x} = Ax + Bu \tag{1}$$

$$y = Cx + Du \tag{2}$$

where the states x are represented by the vector $[\Delta u \quad w \quad q \quad \Delta\theta]^T$, whereas the input is defined as the elevator angle position (for a constant throttle control condition).

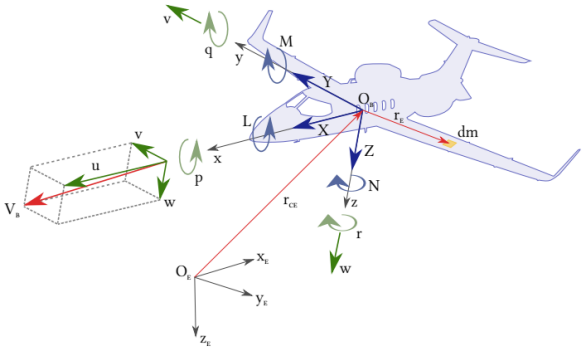

Fig. 1 Aircraft axes definition

The matrices *A, B* and *C* in (1) have the elements presented in (3). The terms $X_u, X_w, Z_u, Z_w, Z_q, Z_{\dot{w}}, M_u, M_q$ and $M_{\dot{w}}$ represent the longitudinal dimensional stability derivatives, and the terms $X_{\delta_e}, Z_{\delta_e}$ and M_{δ_e} define the longitudinal control derivatives. The matrices C and D can be defined depending of the outputs of interest. For the purposes of the present work, C is considered as an identity matrix, and D is a zero matrix. In this format, the outputs considered are as the states previously defined.

The aircraft models implemented in this work are based on the flight data of the model Boeing 747-100, derived from [5], in a cruising and horizontal flight condition at a fixed altitude of 40000 ft (approximately 12192 m) at a Mach Number of 0.8. The original stability and control derivatives of this aircraft model are shown in Table I. This original model was named as model *A*. Based on the original response of this model and in the work developed in [6], two other models were derived: one (named as model *B*) with low proneness to PIO and another (model *C*) with high proneness to the phenomenon. The stability and control derivatives of these models are also shown in Table I, where the same values of the original model are not shown.

TABLE I
MODELS STABILITY AND CONTROL DERIVATIVES

Derivatives	Original (A)	Low (B)	High (C)
X_u	-1.982×10^3	-	-
X_w	4.025×10^3	-	-
Z_u	-2.595×10^4	-	-
Z_w	-9.030×10^4	9.030×10^3	-
Z_q	-4.524×10^5	1.610×10^8	-
$Z_{\dot{w}}$	1.909×10^3	-	-
M_u	1.593×10^4	-	-
M_w	-1.563×10^5	-	-
M_q	-1.521×10^7	-	1.171×10^7
$M_{\dot{w}}$	-1.702×10^4	-	-8.510×10^4
X_{δ_e}	-1.653×10^1	-	-
Z_{δ_e}	-1.579×10^6	6.318×10^7	-3.257×10^8
M_{δ_e}	-5.204×10^7	-5.204×10^8	-

$$A = \begin{bmatrix} \frac{X_u}{m} & \frac{X_w}{m} & 0 & -g\cos\theta_o \\ \frac{Z_u}{m-Z_{\dot{w}}} & \frac{Z_w}{m-Z_{\dot{w}}} & \frac{Z_q+mu_o}{m-Z_{\dot{w}}} & \frac{-mg\ \sin\theta_o}{m-Z_{\dot{w}}} \\ \frac{1}{I_y}\left[M_u + \frac{M_{\dot{w}}Z_u}{(m-Z_{\dot{w}})}\right] & \frac{1}{I_y}\left[M_w + \frac{M_{\dot{w}}Z_u}{(m-Z_{\dot{w}})}\right] & \frac{1}{I_y}\left[M_q + \frac{M_{\dot{w}}(Z_q+mu_o)}{(m-Z_{\dot{w}})}\right] & -\frac{M_{\dot{w}}mg\ \sin\theta_o}{I_y(m-Z_{\dot{w}})} \\ 0 & 0 & 1 & 0 \end{bmatrix}$$

$$B = \begin{bmatrix} \frac{X_{\delta_e}}{m} \\ \frac{Z_{\delta_e}}{m-Z_{\dot{w}}} \\ \frac{M_{\delta_e}}{I_y} + \frac{M_{\dot{w}}}{I_y}\frac{Z_{\delta_e}}{(m-Z_{\dot{w}})} \\ 0 \end{bmatrix} \tag{3}$$

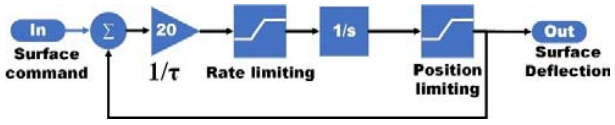

Fig. 2 Aircraft actuator surface model

A more realistic aircraft model can be built by defining a simple representation of the actuator servo-hydraulic of the elevator control surface. This system enables the modeling of the rate and position saturation of the actuators and can be described by the diagram as shown in Fig. 2. In the normal condition of operation, where the system operates far from the extreme positions and velocities, the actuator dynamics can be described by (4). A rate limiting of 40 deg/s and a position limiting of 30 deg/s were set in the present work.

$$G_{ac}(s) = \frac{1}{\tau s+1} \quad (4)$$

III. Control System

The control system applied in this work can be represented by the diagram in Fig. 3. The plant representing the aircraft is implemented applying either the state space models or a commercial flight simulator software in the simulations. The error signal, defined as the difference between the Synthetic Task (Syntask) reference and the actual position of the aircraft, is then sent to the pilot. In this work, the pilot element is represented by a set of transfer function dynamics models. The pilot sends a control signal which is passed to a set of reference state space models. These models consist of a state space equation system, as defined in (1) and (2). Furthermore, these reference models operate in a closed-loop scheme, where the LQR methodology is applied. The outputs of the models are then used in the implementation of a M-MRAC system, which guarantees that the controlled plant modelling the aircraft follows the model reference dynamics. Lastly, the ROVER algorithm detects the PIO phenomenon in real time from the values of the controlled aircraft outputs and of the pilot commands. The ROVER output is then applied in a Gain Scheduling controller, which selects the reference model where output will be sent to the M-MRAC system. In the PIO condition, the low proneness model outputs are sent, and in normal condition, the high or the original proneness models are selected depending of the controlled plant. The next sections describe each of the cited control system elements.

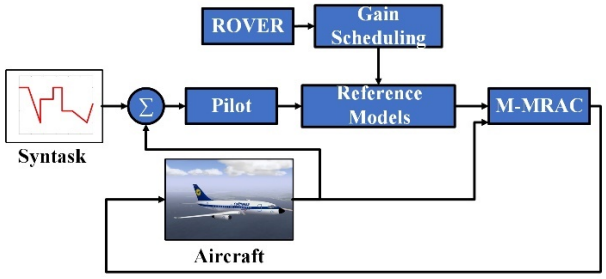

Fig. 3 Control System

A. Pilot Models

Due to the ability to adapt its behavior during the control of an element, the field of modelling the human response consists of a challenging and difficult problem. However, some transfer functions can simulate the human pilot behavior in simple tasks, as the one considered in the present work. For this purpose, three models will be considered: the Tustin [7], the crossover [8] and the precision [9] pilot models described by (5), (6) and (7), respectively. The input for these models is considered as the error e(s) between the reference tracking task and the pitch angle response of the plant, whereas the output of the model is defined as the elevator angle command δp(s). The constant values of these models were obtained from simulations and were chosen with proper values aiming the imposition of a PIO condition in the systems simulated.

$$\frac{\delta_p(s)}{e(s)} = \frac{1.042\times(6.039s+1)e^{-0.617s}}{s} \quad (5)$$

$$\frac{\delta_p(s)}{e(s)} = \frac{6.470\times e^{-0.617s}}{0.156s+1} \quad (6)$$

$$\frac{\delta_p(s)}{e(s)} = 5.964 \times e^{-0.617s}\frac{(1.001s+1)}{(0.887s+1)}G_{NM}(s)$$

$$G_{NM}(s) = \left(\frac{1}{\left(\frac{s^2}{22.292^2}+\frac{2\times 0.8}{22.292}s+1\right)}\right) \quad (7)$$

B. Reference Models: LQR

As stated, the reference models presented in Fig. 3 are defined in a closed loop scheme using the LQR control strategy. This methodology establishes that for a given MIMO system $\dot{x} = Ax + Bu (x \in \mathbb{R}^n \; and \; u \in \mathbb{R}^m)$, a control law in the format $u = -Kx$ must minimize the quadratic cost function:

$$J = \int_0^\infty (x^T Q x + u^T R u) dt \quad (8)$$

where $Q \geq 0$ and $R > 0$ are symmetric, positive semi-definite matrices with appropriated dimensions. The solution for this LQR problem outcomes the gain K in the form:

$$K = R^{-1}B^T P \quad (9)$$

to a $P \in \mathbb{R}^{n\times n}$ positive definite, symmetric matrix which satisfies the equation:

$$PA + A^T P - PBR^{-1}B^T P + Q = 0 \quad (10)$$

Nevertheless, the LQR problem presented here is based on the minimization of a set of signals, commonly known as controlled outputs, in the shortest amount of time. Consequently, some modifications are necessary so as to enable this method to be applied in systems which aim to track a reference signal. One of these methods, as stated in [10], adds to the system a new state z of the error between the reference r and the system output, as follows:

$$\dot{z} = r - C_{lqr}x \quad (11)$$

where C_{lqr} represents a matrix of appropriated dimensions. The system is then altered in an augmented form with the inclusion of this new state:

$$\begin{bmatrix}\dot{x}\\ \dot{z}\end{bmatrix} = \begin{bmatrix}A & 0_{n\times m}\\ -C_{lqr} & 0_{m\times m}\end{bmatrix}\begin{bmatrix}x\\ z\end{bmatrix} + \begin{bmatrix}B\\ 0_{m\times m}\end{bmatrix}u + \begin{bmatrix}0_{n\times m}\\ I_{m\times m}\end{bmatrix}r \quad (12)$$

where I denotes an identity matrix. Once the augmented system is defined as established, a control law which minimizes the quadratic cost function presented in (8) in the format $u = -[K_x \quad K_z]\begin{bmatrix}x\\ z\end{bmatrix}$ is obtained.

C. M-MRAC Controller

The Model Reference Adaptive Control (MRAC) theory establishes a class of controllers where the desired response of

the plant system is specified by a reference model. The parameters of the controller considered are so adjusted based upon the error between the output of the controlled plant and the model reference system. The controller parameters can then converge asymptotically to a set of ideal values, which enable the controlled system to track a reference signal following the dynamics behavior of the reference model.

For a MIMO system, $\dot{x} = Ax + Bu (x \in \mathbb{R}^n \; and \; u \in \mathbb{R}^m)$, with $x(0) = x_0$, a MRAC controller can be stablished applying the inverse Lyapunov theory, as stated in [11]. The main purpose of the these MRAC systems is to obtain a state feedback adaptive control law, so the system state x globally uniformly asymptotically tracks the states $x_{ref} \in \mathbb{R}^n$ of the reference model:

$$\dot{x}_{ref}(t) = A_{ref}x_{ref}(t) + B_{ref}r(t)$$
$$x_{ref}(0) = x_0 \quad (13)$$

where $A_{ref} \in \mathbb{R}^{n \times n}$ defines the Hurwitz matrix, $B_{ref} \in \mathbb{R}^{n \times m}$ and $r(t) \in \mathbb{R}^m$ is an external bounded command vector. The control input u needs to be chosen so that the error presented in (14) globally uniformly asymptotically tends to zero.

$$e(t) = x(t) - x_{ref}(t) \quad (14)$$

Through the application of the inverse Lyapunov theory, the control law can be obtained as stated in (15), where $\widehat{K}_x \in R^{n\,x\,m}$ and $\widehat{K}_r \in R^{m\,x\,m}$ are the control gains (or adaptive laws) generated online by the controller.

$$u = \widehat{K}_x^T x + \widehat{K}_r^T r \quad (15)$$

Considering that the adaptive laws are selected as stated in (16), a Lyapunov function V can be defined, which has its time derivative globally negative semidefinite, in the form $\dot{V} = -e^T Qe \leq 0$ (for some $Q = Q^T > 0$), and with its second derivative bounded in the form $\ddot{V} = -2e^T Q\dot{e}$. Therefore, the Lyapunov analysis states that the state tracking error $e(t)$ defined in (14) tends to the origin globally, uniformly and asymptotically. The terms $\Gamma_x = \Gamma_x^T > 0$ and $\Gamma_r = \Gamma_r^T > 0$ are the rate of adaption matrices and must be selected prior by the user. The matrix $P = P^T > 0$ must satisfy the algebraic Lyapunov equation $PA_{ref} + A_{ref}^T P = -Q$ for some $Q = Q^T > 0$.

$$\dot{\widehat{K}}_x = -\Gamma_x x e^T PB$$
$$\dot{\widehat{K}}_r = -\Gamma_r r(t) e^T PB \quad (16)$$

However, the classical MRAC system here described usually has an oscillatory transient behavior which can deteriorate the controller response and limits its applicability, especially in a PIO scenario, where an oscillatory response already exists. In order to overcome this drawback, a simple modification in the reference model can be made by feeding back the tracking error signal. This approach was named as modified reference model MRAC or M-MRAC and was stablished in [12]. In the M-MRAC system, the tracking error signal $e_m(t) = x(t) - x_m(t)$ is obtained using the modified model reference:

$$\dot{x}_m(t) = A_m x_m(t) + B_m r(t) + \lambda e_m(t)$$
$$x_m(0) = x_0 \quad (17)$$

where $\lambda > 0$ is a design parameter. In this formulation, it can be noticed that for $\lambda = 0$ the conventional MRAC design is obtained again, with $e(t) = e_m(t)$. The application of the Lyapunov stability theory can also prove that the modified state tracking error $e_m(t)$ tends globally, uniformly and asymptotically to the origin. The parameter λ, according to [13] methodology, can be computed in the terms of the adaption rate matrix Γ_r and the matrix P ($P = P^T > 0$ satisfies the algebraic Lyapunov equation $PA_{ref} + A_{ref}^T P = -Q$ for some $Q = Q^T > 0$) as follows:

$$\lambda = \sqrt{2\alpha\Gamma_r \lambda_{máx}(B_m^T P B_m)} \quad (18)$$

where $\alpha = \|x_0\|^2 + sup_t\|r(t)\|^2$ and $\lambda_{máx}$ is an adjustable parameter.

D.Rover

The ROVER algorithm considered in the present work was first defined in [14], and then implemented in some works like [15], [16]. This method can detect in real time the occurrence of the PIO phenomenon by monitoring four parameters: the amplitude and frequency of the pitch rate aircraft response, the amplitude of the pilot command and the phase angle difference between these signals. If each of these parameters exceeds the values presented in Table II, a value of 1 is set to a corresponded flag. Otherwise, they are set with a zero value.

TABLE II
ROVER PARAMETERS

Parameter	Threshold Value
Pitch Rate Magnitude	≥ 8º /s
Pitch rate frequency	0.85 – 10 rad/s
Pilot command	≥ 1.0 (peak-to-peak)
Phase Difference	≥ 40º

E. Gain Scheduling

The schemed called Gain Scheduling denotes a class of control systems where the parameters of the controller are changed by monitoring some operating conditions of the process [17]. The conditions of the process can be fully described by the called scheduling variables. In the present work, the ROVER output and the maximum amplitude of the pitch angular velocity were selected as these variables. This idea is not new in the field of flight control systems and has already been applied in some works like [16]. Thus, the algorithm implemented consists simply in monitoring scheme, where based on the values of the scheduling variables the reference model output is selected and sent to the M-MRAC system. In the PIO condition, the low proneness model outputs are sent whereas in the normal condition the high proneness model (or the original model in the case the controlled process

is defined as the flight simulator software) outputs are sent to the algorithm. The threshold value of the pitch angular velocity in the PIO condition was selected with the value of 17 deg/s peak-to-peak. In order not to lead the system to a high frequency switching between the reference models, a time interval of approximately 5s was defined as the minimal interval where the model of low proneness remains as the reference model.

IV. Methodology

In the first step of this work, simulations were performed using the MATLAB software, considering the state space models *A* as a controlled process. The pilot element was simulated considering the pilot models presented in section III. The simulations were done considering the M-MRAC system firstly acting alone, and then, its integration with the Gain Scheduling suppression technique was simulated.

The second step was done with more simulations performed considering as the controlled system the dynamics model of a Boeing 777-200 aircraft implemented in the flight simulator software FlightGear. The software MATLAB was again applied to allow the integration of the systems considered. The M-MRAC system was applied alone, and then, the suppression system was similarly simulated. The model *A* was applied as the reference model in normal condition and the model *B* in PIO condition and were considered the most accurate pilot models, namely the Tustin and Precision pilot models.

V. Results

Figs. 4-6 present the results obtained from the initial simulations with the M-MRAC system. In this case, the aircraft dynamics is simulated by the state space model *A,* whereas the model *C* was defined as the reference model. In these figures, the ROVER algorithm output as well the PIO level of activation of this output (computed as the total percentage of time of its activation) is also shown. The adaptive suppress system was then simulated and the results achieved are illustrated in Figs. 7-9. In this case, as showed, the system has two reference models, *B* and *C* in PIO and normal condition, respectively. The aircraft dynamics is once more defined by the state model *A* as well the same pilot models were applied. By the use of an analogue procedure, the results shown in Figs. 10 and 11 were obtained from the simulations with the flight simulator software considering the state space model *A* as the reference model in normal condition. Finally, Figs. 12 and 13 present the results obtained from simulations of the suppress system with the Flightgear dynamics model as the controlled plant and model *A* as the reference model in normal condition, whereas model *B* in PIO condition.

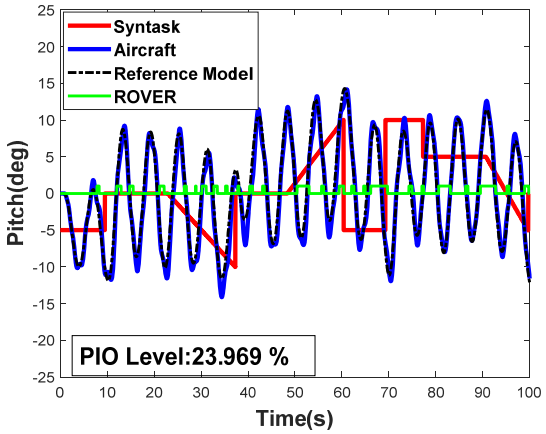

Fig. 4 State Space M-MRAC simulation (Tustin Pilot Model)

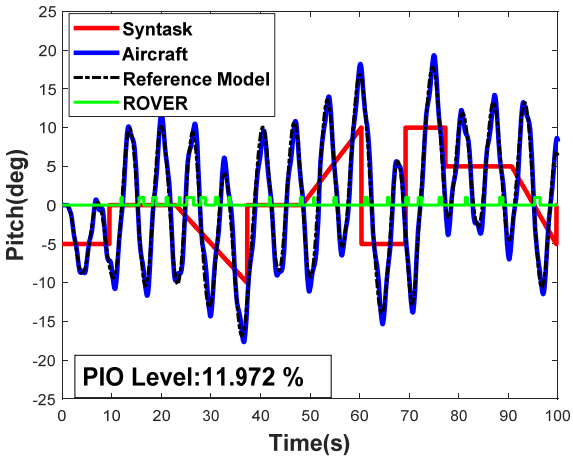

Fig. 5 State Space M-MRAC simulation (Crossover Pilot Model)

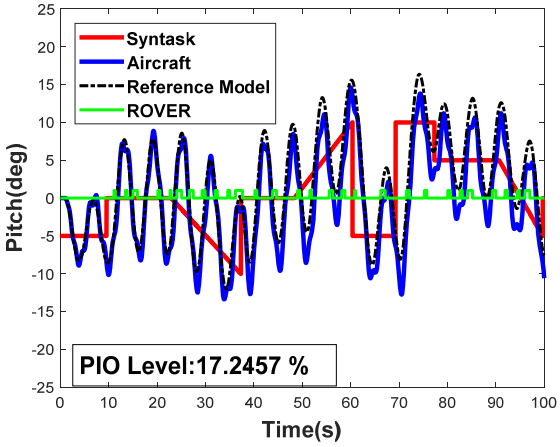

Fig. 6 State Space M-MRAC simulation (Precision Pilot Model)

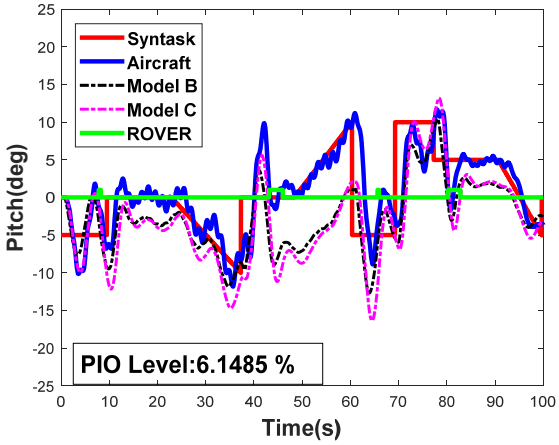

Fig. 7 Suppression state space system simulation (Tustin Pilot Model)

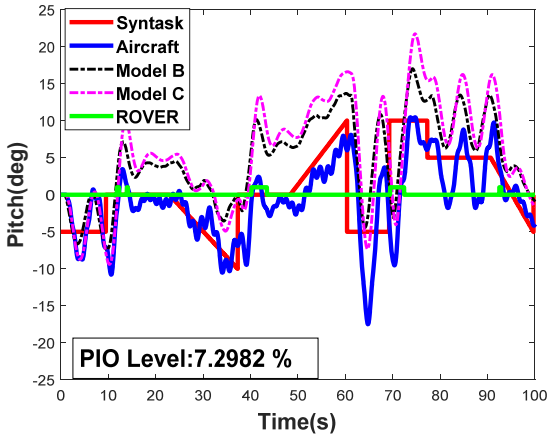

Fig. 8 Suppression state space system simulation (Crossover Pilot Model)

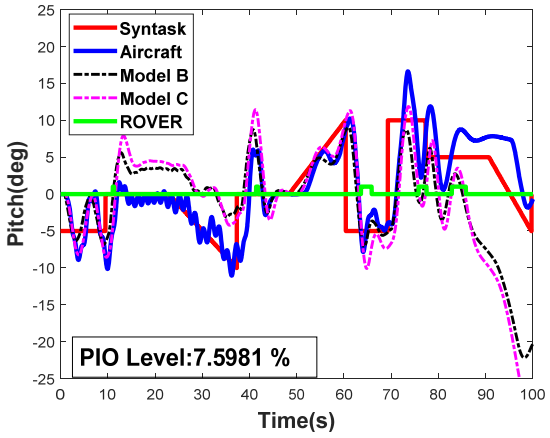

Fig. 9 Suppression state space system simulation (Precision Pilot Model)

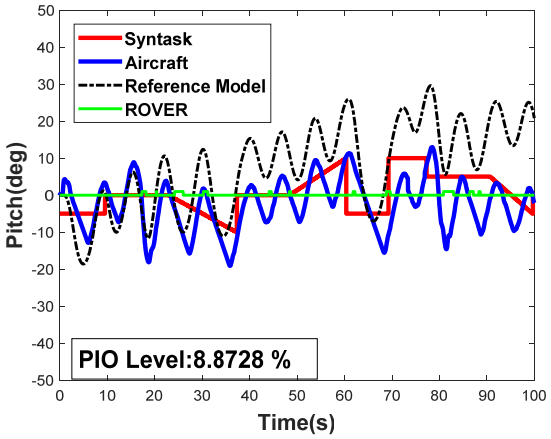

Fig. 10 Flightgear M-MRAC simulation (Tustin Pilot Model)

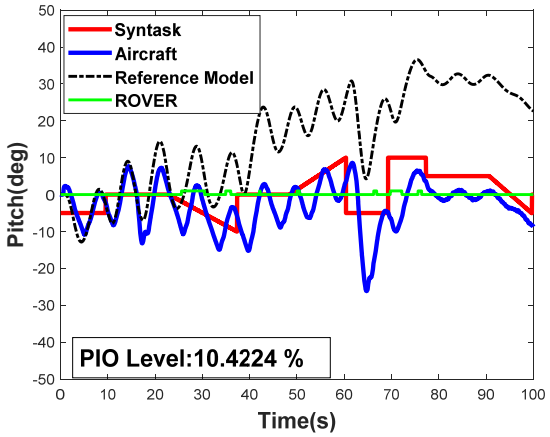

Fig. 11 Flightgear M-MRAC simulation (Precision Pilot Model)

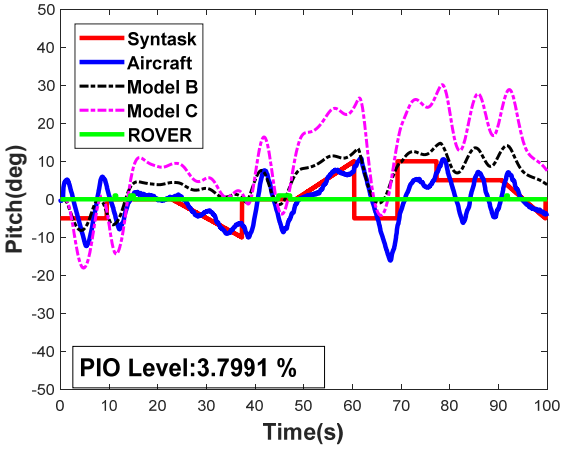

Fig. 12 Suppression Flightgear simulation (Tustin Pilot Model)

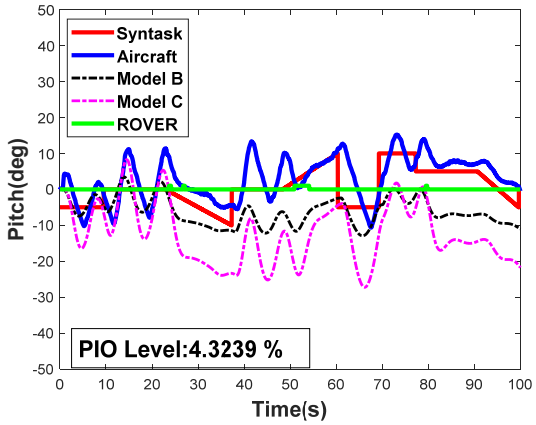

Fig. 13 Suppression Flightgear simulation (Precision Pilot Model)

VI. Discussion

The M-MRAC controller response obtained in the first stage of simulations in the current work, illustrated in Figs. 4-6, showed that the pilot models considered could trigger and sustain PIO oscillations as can be noticed by the ROVER level of activation. Furthermore, the original response of the model *A* could be altered to follow the model *C* dynamics behavior. The suppression system developed was then simulated, considering the same pilot models. As can be seen in Figs. 7-9, this proposed system could suppress (or mitigate) the high amplitude oscillations of PIO. Moreover, the ROVER activation level fell for the three pilot models considered. However, residual oscillations of small amplitude could be noticed in the system response during the suppress phase, where the model of low proneness was working as the reference model. These oscillations are not from the PIO condition but from the M-MRAC dynamics. This behavior can be enhanced by working with higher sample rates, since a small rate of 40 Hz was selected due to MATLAB constraints in simulate real time systems.

In the second stage, the same system was applied in simulations considering as controlled process an aircraft model from a commercial flight simulator. Once more the PIO oscillations could be noticed for the M-MRAC system, as shown in Figs. 10 and 11, with a high level of activation of ROVER algorithm. Furthermore, the proposed controller in this stage could make the flight simulator aircraft to follow the dynamics of the state space model *A*. The suppression system was then applied in the simulations, with the results obtained presented in Figs. 12 and 13. As one can observe, this system could mitigate the high oscillations and lowering the ROVER activation level. Once more the residual oscillations could be suppressed by using a more suitably sample frequency.

VII. Conclusions

The method proposed in this work could mitigate the PIO high amplitude oscillations in the simulations performed. Furthermore, the M-MRAC proposed system could alter the original response of the controlled elements and make them to follow the dynamics of the reference state space models. The ROVER algorithm implemented could also detect in real time of execution the PIO oscillations.

Considering that the system is already integrated with a flight simulator, future works can be performed with trials with human operators, including pilots of different categories and also architectures integrated with movable platforms.

References

[1] Department of Defense Interface Standard. Mil Standard, MIL1797A: Flying qualities of piloted airplanes. Washington D. C., 1995.
[2] I. L. Ashkenas, H. R. Jex, D. T. Mcruer, Pilot-induced oscillations: their cause and analysis. Systems Technology Inc Inglewoodca, 1964.
[3] J. W. Smith, D. T. Berry, Analysis of longitudinal pilot-induced oscillation tendencies of YF-12 aircraft. 1975.
[4] M. R. Anderson, Pilot-induced oscillations involving multiple nonlinearities. Journal of Guidance Control and Dynamics, vol. 21, no. 5, pp. 786- 791, 1998.
[5] B. Etkin, L. D. Reid, Dynamics of flight stability and control, 3rd Edition, pp. 93-128, New York: New York Wiley, 1996.
[6] H. C. Moura, G. S. P. Alegre, J. H. Bidinotto, E. M. Belo, "Pio susceptibility in Fly-By-Wire systems (Accepted for publication)", 31st Congress of the International Council of the Aeronautical Sciences, to be published.
[7] A. Tustin, The nature of the operator's response in manual control, and its implications for controller design. Journal of the Institution of Electrical Engineers-Part IIA: Automatic Regulators and Servo Mechanisms, vol. 94, no. 2, pp. 190-206, 1947.
[8] D. T. Mcruer, E. S. Krendel, Mathematical models of human pilot behavior. Advisory Group for Aerospace Research And Development. Neuilly-SurSeine (France), 1974.
[9] D. T. Mcruer, D. Graham,E. Krendel, W. Reisener, Human pilot dynamics in compensatory systems. Air Force Flight Dynamics. Lab. AFFDL-65-15, 1965.
[10] A. A. Ghaffar, T. Richardson, Model reference adaptive control and LQR control for quadrotor with parametric uncertainties, World Academy of Science, Engineering and Technology, International Journal of Mechanical, Aerospace, Industrial, Mechatronic and Manufacturing Engineering, vol. 9, no. 2, pp. 244-250, 2015.
[11] L., Eugene, W. Kevin, Robust and adaptive control with aerospace applications, 1st Edition, London, Springer, pp. 281-292, 2013.
[12] V. Stepanyan, K. Krishnakumar, MRAC revisited: guaranteed performance with reference model modification, American Control Conference (ACC), IEEE, pp. 93- 98, 2010.
[13] V. Stepanyan, K. Krishnakumar, On the robustness properties of M-MRAC. Infotech@ Aerospace, pp. 2407, 2012.
[14] D. G. Mitchell, A. J. Arencibia, S. Munoz, Real-time detection of pilot-induced oscillations, AIAA Atmospheric Flight Mechanics Conference and Exhibit, Providence, Rhode Island, pp. 4700, 2004.
[15] D. A. Johnson, Suppression of pilot-induced oscillation (PIO). Air force Inst. of Tech Wright-Patterson, Afb. OH School of Engineering and Management, MSc Thesis, 2002.
[16] Q. Liu, Pilot-induced oscillation detection and mitigation, Cranfield University, School of Engineering, Department of Aerospace Engineering, MSc Thesis, 2012.
[17] K. J. Astrom, B.Wittenmark, Adaptive control. 2ª Ed. Reading, Mass: Reading, Mass. Addison-Wesley,1st edition, pp. 390-442, 1934.